Thermodynamics of $Cu_{47}Ti_{34}Zr_{11}Ni_8$, $Zr_{52.5}Cu_{17.9}Ni_{14.6}Al_{10}Ti_5$ and $Zr_{57}Cu_{15.4}Ni_{12.6}Al_{10}Nb_5$ bulk metallic glass forming alloys

S. C. Glade,[a)] R. Busch,[b)] D. S. Lee,[c)] and W. L. Johnson
Division of Engineering and Applied Science, California Institute of Technology, Pasadena, California 91125

R. K. Wunderlich and H. J. Fecht
Materials Science, University of Ulm, Albert-Einstein-Alle 47, D-89081 Ulm, Germany

The differences in the thermodynamic functions between the liquid and the crystalline states of three bulk metallic glass forming alloys, $Cu_{47}Ti_{34}Zr_{11}Ni_8$, $Zr_{52.5}Cu_{17.9}Ni_{14.6}Al_{10}Ti_5$, and $Zr_{57}Cu_{15.4}Ni_{12.6}Al_{10}Nb_5$, were calculated. The heat capacity was measured in the crystalline solid, the amorphous solid, the supercooled liquid, and the equilibrium liquid. Using these heat capacity data and the heats of fusion of the alloys, the differences in the thermodynamic functions between the liquid and the crystalline states were determined. The Gibbs free energy difference between the liquid and the crystalline states gives a qualitative measure of the glass forming ability of these alloys. Using the derived entropy difference, the Kauzmann temperatures for these alloys were determined. © *2000 American Institute of Physics.* [S0021-8979(00)07810-5]

I. INTRODUCTION

Metallic glasses are a relatively new class of materials. They were first obtained from a metallic melt by rapid quenching (approximately $10^6 \, K \, s^{-1}$) in 1961 by Duwez *et al.*[1] Recently, new metallic glass forming compositions have been developed, including La–Al–Ni,[2] Zr–Ni–Al–Cu,[3] Mg–Cu–Y,[4] Zr–Ti–Cu–Ni–Be,[5] and Cu–Ti–Zr–Ni.[6] The best glass former out of these alloys is $Zr_{41.2}Ti_{13.8}Cu_{12.5}Ni_{10}Be_{22.5}$, with a critical cooling rate for glass formation of $1 \, K \, s^{-1}$.[7] Due to the improved glass forming ability of these alloys, experiments on the thermophysical properties in the glassy state and in the supercooled liquid can now be performed, including measurements of specific heat capacity,[8,9] viscosity,[10] atomic diffusion coefficient,[11] and the coefficient of thermal expansion.[12]

In this article, we investigate the thermodynamics of three bulk glass forming alloys: $Cu_{47}Ti_{34}Zr_{11}Ni_8$, $Zr_{52.5}Cu_{17.9}Ni_{14.6}Al_{10}Ti_5$, and $Zr_{57}Cu_{15.4}Ni_{12.6}Al_{10}Nb_5$.[13] With critical cooling rates from 10 to $250 \, K \, s^{-1}$, these alloys have a moderate glass forming ability compared to $Zr_{41.2}Ti_{13.8}Cu_{12.5}Ni_{10}Be_{22.5}$. However, these glasses are among the best nonberyllium containing glasses, making them easier to process and to handle. After measuring the heat capacity of these alloys in the crystalline solid, the amorphous solid, the supercooled liquid, and the equilibrium liquid, the differences in thermodynamic functions between the liquid and the crystalline states can be determined. The Gibbs free energy difference gives a qualitative measure of the stability of the glass compared to the crystalline state.

II. EXPERIMENTAL METHODS

We prepared the alloys in an arc melter with a titanium gettered, ultrahigh purity argon atmosphere, with elements of purities from 99.9% to 99.9999%. The nominal compositions of the alloys prepared were $Cu_{47}Ti_{34}Zr_{11}Ni_8$, $Zr_{52.5}Cu_{17.9}Ni_{14.6}Al_{10}Ti_5$, and $Zr_{57}Cu_{15.4}Ni_{12.6}Al_{10}Nb_5$. To obtain amorphous samples for differential scanning calorimetry (DSC) experiments, we melted the alloys in quartz tubes in a radio frequency induction furnace and then injection cast the melt with argon into a copper mold. The molten metals were held in the quartz tubes for as short a time as possible (usually <10 s) to avoid any contamination.

In previous work done on SiC composites with $Cu_{47}Ti_{34}Zr_{11}Ni_8$ and $Zr_{57}Cu_{15.4}Ni_{12.6}Al_{10}Nb_5$ as the matrix material, silicon additions to the alloy improved the thermal stability of the amorphous solid.[14,15] We do not see this improvement in the thermal stability of the amorphous solid, so the silicon contamination from melting these alloys in quartz tubes is thought to be less than 0.5% atomic.

A DSC (Perkin Elmer DSC-7) was used to determine the absolute specific heat capacity of the alloys. Heating a sample at $0.333 \, K \, s^{-1}$ and then holding it at a constant temperature results in a step in heat flux given by

$$\dot{Q} = \frac{\partial Q}{\partial t} = \left(\frac{\partial Q}{\partial t}\right)_{\dot{T} \neq 0} - \left(\frac{\partial Q}{\partial t}\right)_{\dot{T}=0} = c \cdot \frac{dT}{dt}, \quad (1)$$

where $(\partial Q/\partial t)_{\dot{T} \neq 0}$ is the power required to heat the sample and sample pan at a constant heating rate, $(\partial Q/\partial t)_{\dot{T}=0}$ is the power needed to hold the sample and sample pan at a con-

a)Author to whom correspondence should be addressed; electronic mail: sglade@caltech.edu
b)Current address: Department of Mechanical Engineering, Oregon State University, Corvallis, OR 97331.
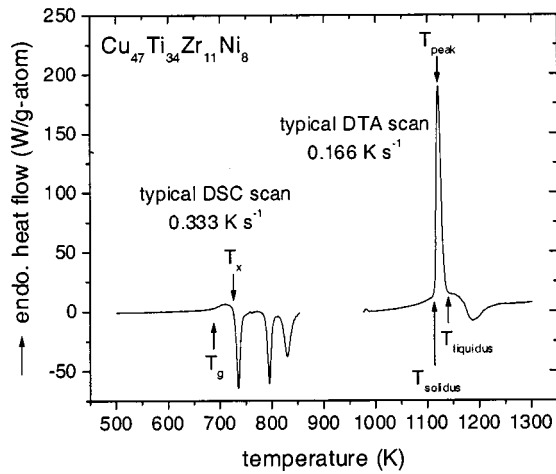c)Current address: Symyx Technologies, Santa Clara, CA 95051.

FIG. 1. Thermal behavior of $Cu_{47}Ti_{34}Zr_{11}Ni_8$ upon heating. The lower temperature data were obtained with a DSC (heating rate of 0.333 K s^{-1}) and the higher temperature data were obtained with a DTA (heating rate of 0.167 K s^{-1}). The onset of the glass transition, T_g, the onset of crystallization, T_x, the solidus temperature, $T_{solidus}$, the temperature at the peak of the melting endotherm, T_{peak}, and the liquidus temperature, $T_{liquidus}$, are indicated. The exothermic hump after the melting peak is due to the reaction of the alloy with the graphite crucible.

stant temperature, and c is the heat capacity of the sample and sample pan. By performing these heat flux steps every 20 K on the metal sample in the sample pan, a sapphire standard in the sample pan, and the sample pan by itself, the absolute specific heat capacity of the metal sample can be determined by

$$c_p(T)_{metal} = \frac{\dot{Q}_{metal} - \dot{Q}_{pan}}{\dot{Q}_{sapphire} - \dot{Q}_{pan}} \cdot \frac{m_{sapphire} \cdot \mu_{metal}}{m_{metal} \cdot \mu_{sapphire}}$$
$$\cdot c_p(T)_{sapphire}, \tag{2}$$

where m_i is mass, μ_i is molar mass, and $c_p(T)_{sapphire}$ is the heat capacity of sapphire.[9]

The absolute specific heat capacity of the supercooled liquid immediately after the glass transition could not be measured using the method described above because these alloys are not very stable against crystallization in this temperature range. To determine the specific heat capacity in this

TABLE I. Glass transition temperatures, crystallization temperatures, solidus temperatures, peak temperatures (peak of the melting endotherm), liquidus temperatures, and the heats of fusion for the three alloys. The solidus and liquidus temperatures of $Cu_{47}Ti_{34}Zr_{11}Ni_8$ measured in this study differ from the previously reported values of 1105 and 1160 K, respectively (see Ref. 6). Lin performed DTA experiments using alumina crucibles, while we performed the DTA experiments using graphite crucibles. The difference in the values measured is attributed to the reaction of the alloy with the alumina crucibles.

	T_g[a] (K)	T_x[a] (K)	$T_{solidus}$[b] (K)	T_{peak}[b] (K)	$T_{liquidus}$[b] (K)	ΔH_f[b] (kJ g atom^{-1})
$Cu_{47}Ti_{34}Zr_{11}Ni_8$	673	717	1114	1119	1128	11.3
$Zr_{52.5}Cu_{17.9}Ni_{14.6}Al_{10}Ti_5$	675	727	1072	1085	1091	8.2
$Zr_{57}Cu_{15.4}Ni_{12.6}Al_{10}Nb_5$	682	742	1091	1105	1115	9.4

[a]Measured with a heating rate of 0.333 K s^{-1}.
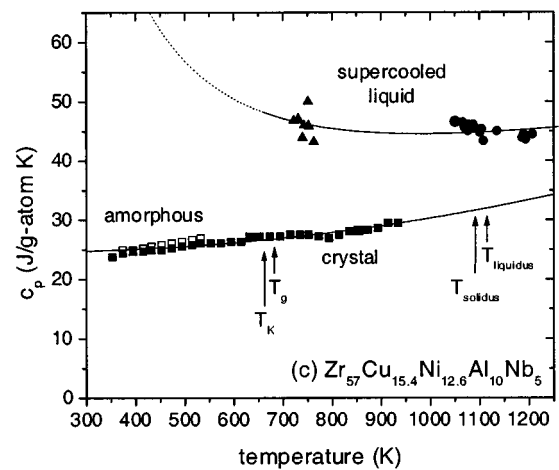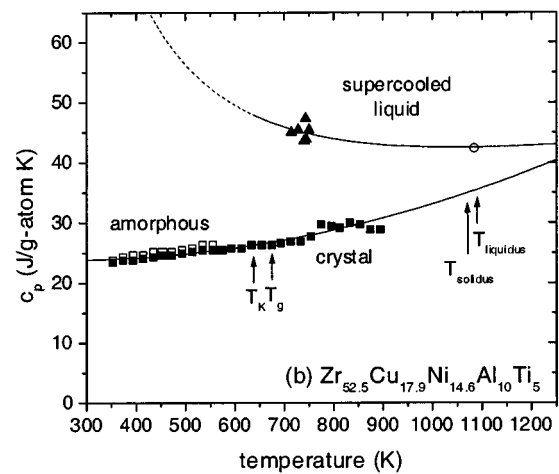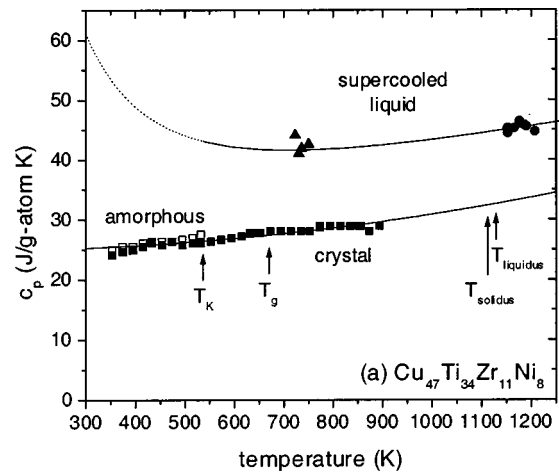[b]Measured with a heating rate of 0.167 K s^{-1}.

FIG. 2. The specific heat capacity of the crystalline solid (■), the amorphous alloy (□), the supercooled liquid measured with constant heating rate experiments (▲), and the undercooled liquid and the equilibrium liquid measured with ac modulation calorimetry (●) for: (a) $Cu_{47}Ti_{34}Zr_{11}Ni_8$, (b) $Zr_{52.5}Cu_{17.9}Ni_{14.6}Al_{10}Ti_5$, and (c) $Zr_{57}Cu_{15.4}Ni_{12.6}Al_{10}Nb_5$. For $Zr_{52.5}Cu_{17.9}Ni_{14.6}Al_{10}Ti_5$, the equilibrium liquid data were not measured, but a value of 42.5 J g atom^{-1} K^{-1} at 1085 K was assigned to allow the determination of the fitting constant for the liquid specific heat capacity (○). The lines on the graphs are the fits to Eqs. (7) and (8).

TABLE II. Fitting constants for the heat capacity data, using $c_{p,\text{crystal}}(T)=3R+aT+bT^2$ to fit the crystalline state heat capacity data and $c_{p,\text{liquid}}(T)=3R+cT+dT^{-2}$ to fit the liquid heat capacity data.

	a (J g atom^{-1} K^{-2})	b (J g atom^{-1} K^{-3})	c (J g atom^{-1} K^{-2})	d (J g atom^{-1} K)
$Cu_{47}Ti_{34}Zr_{11}Ni_8$	−0.000 89	6.82×10^{-6}	0.0156	2.83×10^6
$Zr_{52.5}Cu_{17.9}Ni_{14.6}Al_{10}Ti_5$	−0.008 61	16.8×10^{-6}	0.0112	6.43×10^6
$Zr_{57}Cu_{15.4}Ni_{12.6}Al_{10}Nb_5$	−0.003 02	8.37×10^{-6}	0.0133	6.32×10^6

temperature range, constant heating rate DSC experiments were performed at 0.333, 0.667, 1.33, and 3.33 K s^{-1}. The specific heat capacity is determined by

$$c_{p,\text{glass}}=\frac{\dot{Q}\mu}{\dot{T}m}+c_{p,\text{crystal}}+\text{scaling constant}, \quad (3)$$

where $\dot{Q}$ is the power input, $\dot{T}$ is the heating rate, m is the mass, and μ is the molar mass. The DSC was calibrated for each heating rate to account for the shift in temperature with different heating rates.

Alternating current (ac) modulation calorimetry[16,17] was used to measure the specific heat capacity of the undercooled liquid and the equilibrium liquid. The ac modulation calorimetry technique was performed using TEMPUS (Tiegelfreies Elektromagnetisches Prozessieren Unter Schwerelosigkeit, see Ref. 18), an electromagnetic processing facility that flew on board the National Aeronautics and Space Administration's (NASA) space shuttle. ac modulation calorimetry is a noncontact technique for measuring heat capacity; by modulating the power input to the sample and measuring the temperature response, the heat capacity can be determined. Two time constants are important in this experimental method:

$$\tau_1=\frac{c_p}{4A\epsilon_T\sigma T_0^3} \quad (4)$$

and

$$\tau_2=\frac{3c_p}{4\pi^3R\kappa_{\text{th}}}, \quad (5)$$

where c_p is the sample heat capacity, A is the sample surface area, ϵ_T is the total hemispherical emissivity of the sample surface, σ is the Stefan–Boltzman constant, T_0 is the sample temperature, R is the sample radius, and κ_{th} is the sample thermal conductivity. τ_1 is the external relaxation time due to radiative heat loss and τ_2 is the internal relaxation time due to the finite thermal conductivity of the sample. Heat capacity is determined by

$$c_p=f(\omega,\tau_1,\tau_2)\frac{P_m(\omega)}{\Delta T_m(\omega)\omega}, \quad (6)$$

where f is a correction function for radiation loss and finite thermal conductivity, $P_m(\omega)$ is the power of modulation, $\Delta T_m(\omega)$ is the amplitude of temperature response to the power modulation, and ω is the frequency of modulation. Modulation frequencies of 0.08 and 0.12 Hz were used in these experiments.

A differential thermal analyzer (Perkin Elmer DTA-7), using a heating rate of 0.167 K s^{-1}, was used to determine the heats of fusion, the solidus temperatures, and the liquidus temperatures of these alloys. Graphite crucibles were used in these experiments to minimize the reaction between the molten alloy and crucible.

III. RESULTS

Upon heating an amorphous alloy at a constant heating rate, the alloy goes through the glass transition, crystallizes, and then melts. This behavior is shown in Fig. 1, a DSC scan and a differential thermal analysis (DTA) scan of $Cu_{47}Ti_{34}Zr_{11}Ni_8$. The onset of the glass transition T_g is indicated by a small endothermic rise. Crystallization begins at $T_x=717$ K, with three exothermic peaks. $Zr_{52.5}Cu_{17.9}Ni_{14.6}Al_{10}Ti_5$ and $Zr_{57}Cu_{15.4}Ni_{12.6}Al_{10}Nb_5$ both have a single crystallization peak after heating through the glass transition. For $Cu_{47}Ti_{34}Zr_{11}Ni_8$, melting begins at the solidus temperature of 1114 K, with the alloy being completely molten at the liquidus temperature of 1128 K. Integrating the area of the melting peak, we find that the heat of fusion is 11.3 kJ g atom^{-1} for $Cu_{47}Ti_{34}Zr_{11}Ni_8$. The characteristic temperatures as well as the heats of fusion of $Cu_{47}Ti_{34}Zr_{11}Ni_8$ and the other two alloys, $Zr_{52.5}Cu_{17.9}Ni_{14.6}Al_{10}Ti_5$ and $Zr_{57}Cu_{15.4}Ni_{12.6}Al_{10}Nb_5$, are summarized in Table I.

The specific heat capacity of the crystalline solid, the amorphous solid, the supercooled liquid, and the equilibrium liquid for each alloy is shown in Figs. 2(a)–2(c). The specific heat capacity for the crystalline and the amorphous states was determined by DSC experiments, while the specific heat capacity of the undercooled liquid and the equilibrium liquid was determined by ac modulation calorimetry. Since the amorphous solid is not in thermodynamic equilibrium or metastable equilibrium in the glass transition region, heat capacity data in this region are not included.

The heat capacity of a crystal well above the Debye temperature can be described by[19]

$$c_{p,\text{crystal}}(T)=3R+aT+bT^2. \quad (7)$$

The heat capacity of an undercooled liquid can be described by

$$c_{p,\text{liquid}}(T)=3R+cT+dT^{-2}, \quad (8)$$

where $R=8.314\,52$ J g atom^{-1} K^{-1}, and a, b, c, and d are fitting constants. The constants for both fits to the specific heat capacity data for each alloy are summarized in Table II.
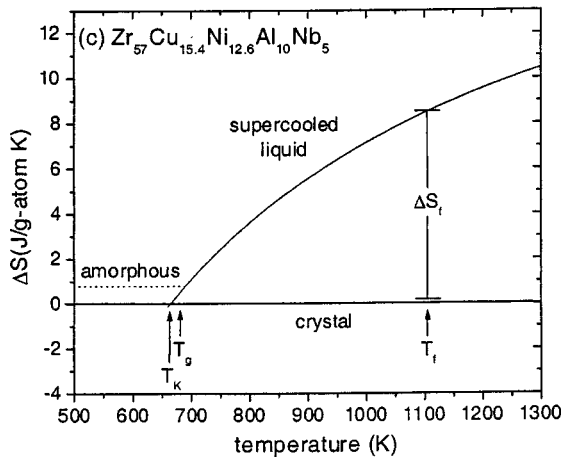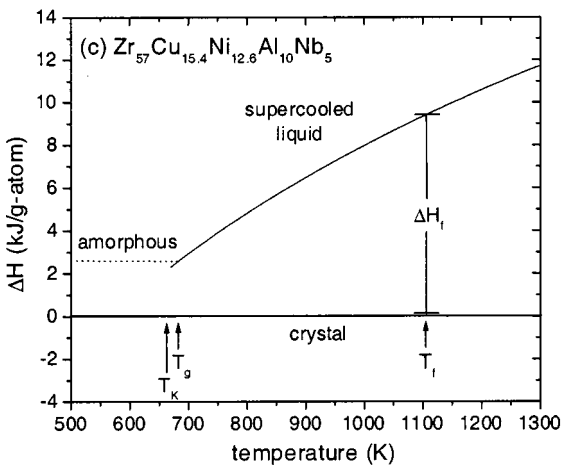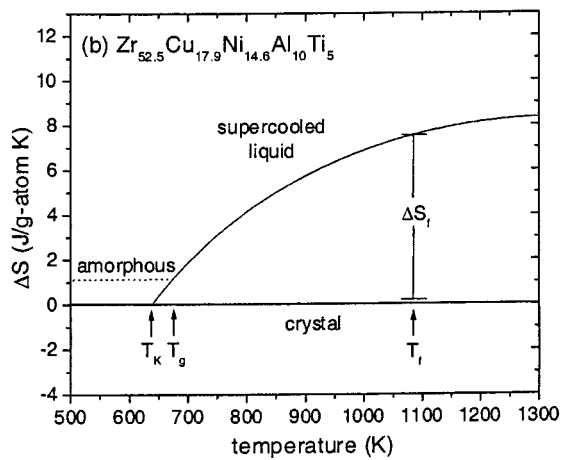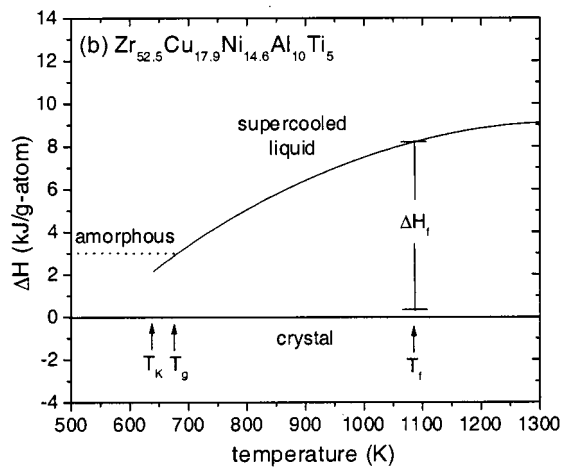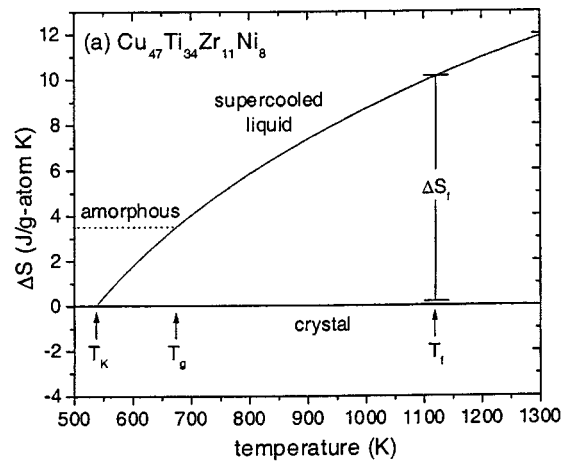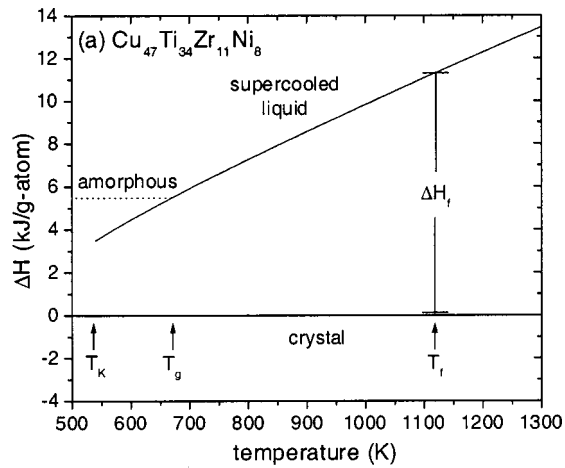
FIG. 3. The calculated difference in enthalpy between the liquid and the crystalline states as a function of temperature for (a) $Cu_{47}Ti_{34}Zr_{11}Ni_8$, (b) $Zr_{52.5}Cu_{17.9}Ni_{14.6}Al_{10}Ti_5$, and (c) $Zr_{57}Cu_{15.4}Ni_{12.6}Al_{10}Nb_5$. Also indicated on these plots are the Kauzmann temperature T_K, the glass transition temperature T_g (onset with a heating rate of 0.333 K s^{-1}), and the temperature at which the Gibbs free energy of the liquid and the crystalline states are taken to be equal, T_f.

FIG. 4. The calculated difference in entropy between the liquid and the crystalline states for (a) $Cu_{47}Ti_{34}Zr_{11}Ni_8$, (b) $Zr_{52.5}Cu_{17.9}Ni_{14.6}Al_{10}Ti_5$, and (c) $Zr_{57}Cu_{15.4}Ni_{12.6}Al_{10}Nb_5$. Indicated on these plots are the Kauzmann temperature T_K, the glass transition temperature T_g (onset with a heating rate of 0.333 K s^{-1}), and the temperature at which the Gibbs free energy of the liquid and the crystalline states are taken to be equal T_f.

The specific heat capacity of $Zr_{52.5}Cu_{17.9}Ni_{14.6}Al_{10}Ti_5$ in the undercooled liquid and equilibrium liquid was not measured with ac modulation calorimetry. However, the specific heat capacity of the liquid for many metallic glass forming alloys, including $Zr_{41.2}Ti_{13.8}Cu_{12.5}Ni_{10}Be_{22.5}$,[8] and $Mg_{65}Cu_{25}Y_{10}$,[9] is approximately 40 J g atom^{-1} K^{-1} at the melting temperature. For $Cu_{47}Ti_{34}Zr_{11}Ni_8$ and $Zr_{57}Cu_{15.4}Ni_{12.6}Al_{10}Nb_5$ (this work), the heat capacity near the melting temperature is approximately 45 J g atom^{-1} K^{-1}.

TABLE III. The Kauzmann temperatures, the glass transition temperatures (measured with a heating rate of 0.333 K s^{-1}), and the entropies of fusion for the three alloys.

	T_K (K)	T_g (K)	ΔS_f (J g atom^{-1} K^{-1})
Cu$_{47}$Ti$_{34}$Zr$_{11}$Ni$_8$	537	673	10.1
Zr$_{52.5}$Cu$_{17.9}$Ni$_{14.6}$Al$_{10}$Ti$_5$	638	675	7.6
Zr$_{57}$Cu$_{15.4}$Ni$_{12.6}$Al$_{10}$Nb$_5$	664	682	8.5

Therefore, a specific heat capacity of 42.5 J g atom^{-1} K^{-1} at 1085 K was assigned to Zr$_{52.5}$Cu$_{17.9}$Ni$_{14.6}$Al$_{10}$Ti$_5$, so that the fitting constants for the liquid specific heat capacity could be determined. It is expected that this value is within 10% of the actual value.

The difference in the specific heat capacity of the liquid and the crystalline states, Δc_p^{l-x}, was calculated. With these data, the differences in the thermodynamic functions of the liquid and the crystalline states can be determined. The calculated difference in enthalpy is given by

$$\Delta H^{l-x}(T) = \Delta H_f - \int_T^{T_f} \Delta c_p^{l-x}(T') dT' \quad (9)$$

and is shown in Figs. 3(a)–3(c) for these alloys. In this equation, ΔH_f is the enthalpy of fusion and T_f is the temperature at which the Gibbs free energy of the liquid and the crystalline states are equal. The difference in the enthalpy between the liquid and the crystalline states at the glass transition (measured with a rate of 0.333 K s^{-1}) is the amount of enthalpy frozen into the liquid at T_g.

T_f, the temperature at which the Gibbs free energy of the liquid and the crystalline states are equal, is not known exactly for these alloys. However, the Gibbs free energy of the liquid and the crystalline states are equal to one another between the solidus and liquidus temperatures. T_f was taken to be the temperature at which the endothermic peak is maximum during melting (determined with the DTA), T_{peak}, as listed in Table I.

The calculated difference in entropy between the liquid and crystalline states is given by

$$\Delta S^{l-x}(T) = \Delta S_f - \int_T^{T_f} \frac{\Delta c_p^{l-x}(T')}{T'} dT' \quad (10)$$

and is shown in Figs. 4(a)–4(c) for these alloys. T_{peak} is used in place of T_f in this calculation. ΔS_f, the entropy of fusion, is given by

$$\Delta S_f = \frac{\Delta H_f}{T_f}. \quad (11)$$

Entropy of fusion data are found in Table III. Similar to the $\Delta H^{l-x}(T)$ function that was calculated, there is residual entropy frozen into the glass below the glass transition temperature. The T_K indicated on these plots is the calculated Kauzmann temperature. The Kauzmann temperature is the isentropic temperature, the temperature at which the entropy of the liquid is equal to the entropy of the crystal. This temperature is commonly believed to be the lowest temperature at which a supercooled liquid can exist without either spon-
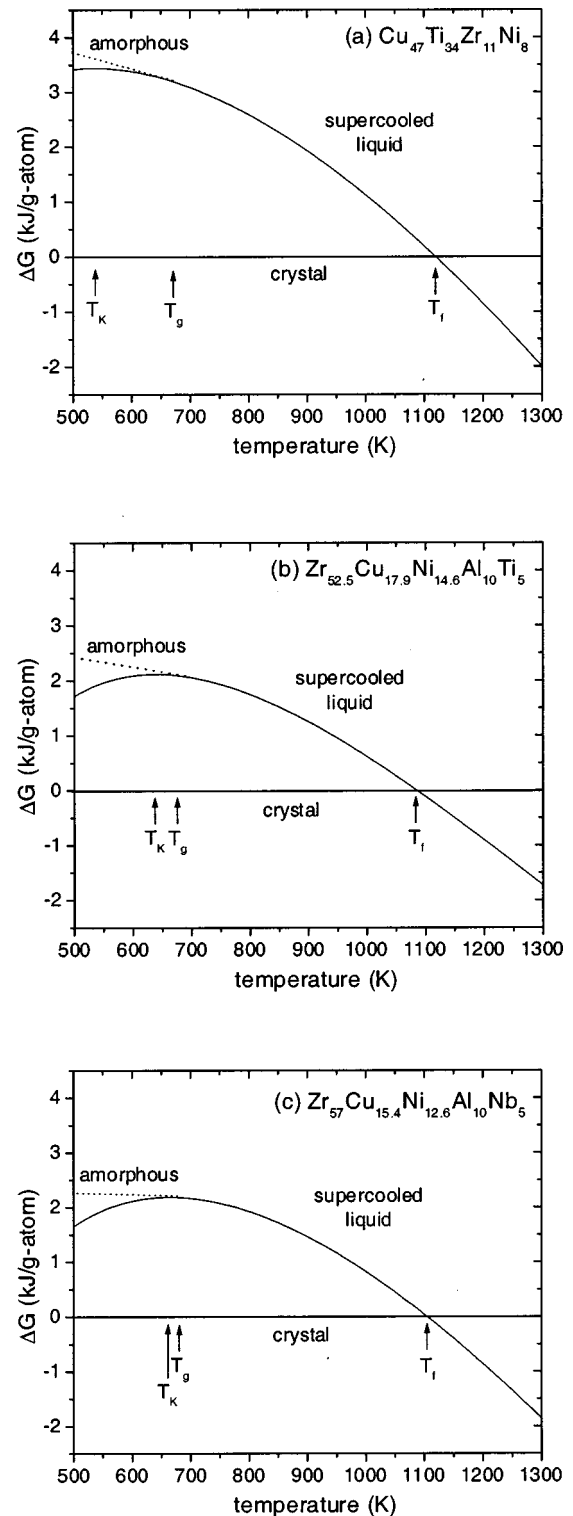

FIG. 5. The calculated difference in the Gibbs free energy between the liquid and the crystalline states for (a) Cu$_{47}$Ti$_{34}$Zr$_{11}$Ni$_8$, (b) Zr$_{52.5}$Cu$_{17.9}$Ni$_{14.6}$Al$_{10}$Ti$_5$, and (c) Zr$_{57}$Cu$_{15.4}$Ni$_{12.6}$Al$_{10}$Nb$_5$. Indicated on these plots are the Kauzmann temperature T_K, the glass transition temperature T_g (onset with a heating rate of 0.333 K s^{-1}), and the temperature at which the Gibbs free energy of the liquid and the crystalline states are taken to be equal T_f.

taneously crystallizing or forming a glass.[20] Kauzmann temperature data are found in Table III. It is important to note that the entropy difference that is calculated from the heat capacity data is the total entropy difference between the liq-

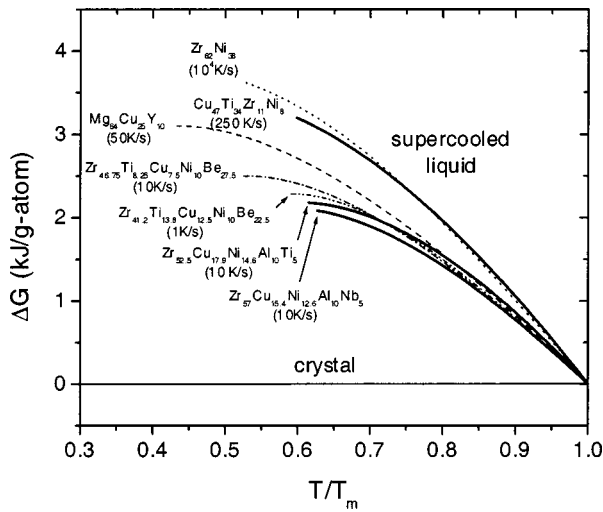J. Appl. Phys., Vol. 87, No. 10, 15 May 2000

Glade *et al.*   7247

FIG. 6. The calculated difference in the Gibbs free energy between the liquid and the crystalline states for a number of glass forming alloys (see Ref. 9).

TABLE IV. The critical cooling rates and the reduced glass transition temperatures for the three alloys in this work and two other metallic glass forming alloys, in order of decreasing glass forming ability.

	Critical cooling rate (K s^{-1})	T_{rg}[a]
$Zr_{41.2}Ti_{13.8}Cu_{12.5}Ni_{10}Be_{22.5}$[b]	1	0.67
$Zr_{57}Cu_{15.4}Ni_{12.6}Al_{10}Nb_5$	10	0.62
$Zr_{52.5}Cu_{17.9}Ni_{14.6}Al_{10}Ti_5$	10	0.62
$Mg_{65}Cu_{25}Y_{10}$[c]	50	0.59
$Cu_{47}Ti_{34}Zr_{11}Ni_8$	250	0.60

[a]Determined using the onset of the glass transition measured with a heating rate of 0.333 K s^{-1} and the liquidus temperature measured with a heating rate of 0.167 K s^{-1}.
[b]See Ref. 8.
[c]See Ref. 9.

uid and the crystalline states and not the configurational entropy difference. The total entropy difference between the liquid and the crystalline states includes configurational entropy, communal entropy, and vibrational entropy. Thus, this calculated Kauzmann temperature does not necessarily represent the temperature where the configurational entropy of the liquid vanishes.

The calculated difference in the Gibbs free energy between the liquid and crystalline states is given by

$$\Delta G^{l-x}(T) = \left(\Delta H_f - \int_T^{T_f} \Delta c_p^{l-x}(T')dT' \right)$$
$$- T\left(\Delta S_f - \int_T^{T_f} \frac{\Delta c_p^{l-x}(T')}{T'} dT' \right) \quad (12)$$

and is shown in Figs. 5(a)–5(c) for these alloys.

IV. DISCUSSION

A comparison of the Gibbs free energy difference between the liquid and the crystal for several metallic glass forming alloys[9] is shown in Fig. 6, along with the estimated critical cooling rates for these alloys. In general, the lower the Gibbs free energy difference between the liquid and the crystalline states, the better the glass forming ability of the alloy (according to the critical cooling rate). It is important to note that this Gibbs free energy difference is the driving force for crystallization only in the case of a polymorphic transformation. If the crystallization is not polymorphic (as is the case for many metallic glass forming compositions), this free energy difference is the lower limit of the thermodynamic driving force for crystallization.

Also, in general, the smaller the entropy of fusion, the better is the glass forming ability of these metallic glasses. This is understood by the Turnbull approximation[21]

$$\Delta G^{l-x} = \Delta H_f - T\Delta S_f, \quad (13)$$

which is a good approximation immediately below the melting point. Initially, as the liquid is undercooled, the entropy of fusion ΔS_f determines the rate at which ΔG^{l-x} changes.

Another parameter that is a qualitative indicator of the glass forming ability in glass forming alloys is the reduced glass transition temperature T_{rg}. The reduced glass transition temperature is given by

$$T_{rg} = \frac{T_g}{T_m}, \quad (14)$$

where T_g is the glass transition temperature and T_m is the melting temperature. It is a measure of the time spent in the supercooled liquid regime when cooling the liquid from the melt. Larger reduced glass transition temperatures indicate better glass forming ability; the temperature interval between the melting temperature and glass transition temperature is smaller, decreasing the likelihood of crystallization. Values of the critical cooling rates and T_{rg} for the three alloys in this work and two other metallic glass forming alloys are given in Table IV.

V. SUMMARY AND CONCLUSION

The thermodynamic functions of three bulk glass forming alloys, $Cu_{47}Ti_{34}Zr_{11}Ni_8$, and $Zr_{52.5}Cu_{17.9}Ni_{14.6}Al_{10}Ti_5$, and $Zr_{57}Cu_{15.4}Ni_{12.6}Al_{10}Nb_5$, were determined. To do this, the heat capacity in the crystalline solid, the amorphous solid, the supercooled liquid, and the equilibrium liquid, and the heats of fusion for these alloys were measured. The Gibbs free energy difference between the liquid and the crystalline states gives a qualitative measure of the glass forming ability of these glass forming alloys.

[1] W. Klement, R. H. Willens, and P. Duwez, Nature (London) **187**, 869 (1960).

[2] A. Inoue, T. Zhang, and T. Masumoto, Mater. Trans., JIM **31**, 425 (1990).

[3] T. Zhang, A. Inoue, and T. Masumoto, Mater. Trans., JIM **32**, 1005 (1991).

[4] A. Inoue, A. Kato, T. Zhang, S. G. Kim, and T. Masumoto, Mater. Trans., JIM **32**, 609 (1991).

[5] A. Peker and W. L. Johnson, Appl. Phys. Lett. **63**, 2342 (1993).

[6] X. H. Lin and W. L. Johnson, J. Appl. Phys. **78**, 6514 (1995).

[7] Y. J. Kim, R. Busch, W. L. Johnson, A. J. Rullison, and W. K. Rhim, Appl. Phys. Lett. **65**, 2136 (1994).

[8] R. Busch, Y. J. Kim, and W. L. Johnson, J. Appl. Phys. **77**, 4039 (1995).

[9] R. Busch, W. Liu, and W. L. Johnson, J. Appl. Phys. **83**, 4134 (1998).

[10] A. Masuhr, R. Busch, and W. L. Johnson, J. Non-Cryst. Solids **252**, 566 (1999).

[11] U. Geyer, S. Schneider, W. L. Johnson, Y. Qui, T. A. Tombrello, and M. P. Macht, Phys. Rev. Lett. **75**, 2364 (1995).

[12] K. Ohsaka, S. K. Chung, W. K. Rhim, A. Peker, D. Scruggs, and W. L. Johnson, Appl. Phys. Lett. **70**, 726 (1997).

[13] X. H. Lin, Ph.D. thesis, California Institute of Technology, 1997.

[14] H. Choi-Yim, R. Busch, and W. L. Johnson, J. Appl. Phys. **83**, 7993 (1998).

[15] H. Choi-Yim, R. Busch, U. Köster, and W. L. Johnson, Acta Mater. **47**, 2455 (1999).

[16] H. J. Fecht and W. L. Johnson, Rev. Sci. Instrum. **62**, 1299 (1991).

[17] R. K. Wunderlich and H. J. Fecht, Int. J. Thermophys. **17**, 1203 (1996).

[18] J. Szekely, E. Schwartz, and R. Hyers, JOM **47**, 50 (1995).

[19] O. Kubaschewski, C. B. Alcock, and P. J. Spencer, *Materials Thermochemistry*, 6th ed. (Permagon, New York, 1993).

[20] W. Kauzmann, Chem. Rev. **43**, 219 (1948).

[21] D. Turnbull, J. Appl. Phys. **21**, 1022 (1950).